ELSEVIER

Thermochimica Acta 282/283 (1996) 175–189

thermochimica acta

Thermal analysis of the oxygen activity and electrical resistance in the 2212 and 2223 compositions of the $(Bi, Pb)_2 Sr_2 Ca_{n-1} Cu_n O_x$ isopleth[1]

J. Hertz[a,*], M. Nassik[a], M. Mansori[b], P. Satre[b], A. Sebaoun[b]

[a] *Laboratoire de Thermodynamique Métallurgique URA 158, Université Henri Poincaré, Nancy 1, Faculté des Sciences, B.P. 239, 54506 Vandoeuvre-les-Nancy Cedex, France*

[b] *Laboratoire de Physico-Chimie des Matériaux et du Milieu Marin, Université de Toulon et du Var, Equipe Matériaux à Finalités Spécifiques E.A. 1356, Faculté des Sciences et Technique B.P. 132, 83957 La Garde Cedex, France*

Abstract

Phase transformations in Pb-2212 and Pb-2223 compositions contained in the isopleth defined by the formula $(Bi, Pb)_2 Sr_2 Ca_{n-1} Cu_n O_{2n+4+\delta}$ were investigated by thermal analysis of the oxygen activity and of the electrical resistance, inside an electrolytic cell of CaO-stabilized zirconia.

These methods of thermal analysis allow us to not only determine the main known phase transformations in these compositions but also new transformations in the system close to 750°C and 500°C under $p(O_2) = 10^5$ Pa pure oxygen atmosphere. Our e.m.f. thermal analysis shows the existence of a strong redox equilibrium spread between 300 and 550°C which was also detected by the resistance analysis and cannot be interpreted by a phase transformation. X-ray diffraction analysis has proved that no structural transformation appears below 550°C. The results obtained in both parts of the 750°C transformation by X-ray diffraction of quenched powders are still too incomplete to conclude that the Majewski eutectoïd transition: $2212 \leftrightarrow 2201 + 1/2\,Ca_2CuO_3 + 1/2\,CuO$ occurs at this temperature but this transformation might correspond to $(Ca, Sr)_2PbO_4$ precipitation.

Both the new redox transformations observed arround 750 and 500°C might also be valence transitions, inside the high-T_c superconducting phases.

Keywords: $(Bi, Pb)_2 Sr_2Ca_{n-1} Cu_n O_{2n+4+\delta}$; Electrical resistance; Isopleth; Oxygen activity; Phase transformation; Redox transformation; Thermal analysis; X-ray diffraction

* Corresponding author.

[1] Dedicated to Takeo Ozawa on the Occasion of his 65th Birthday.

SSDI 0040-6031(96)02816-X

1. Introduction

In the lead-doped Bi_2O_3–SrO–CaO–CuO system, three high T_c superconducting phases were reported and identified as compounds of the homologous series $(Bi, Pb)_2 Sr_2 Ca_{n-1} Cu_n O_{2n+4+\delta}$ where n is the number of CuO_2 planes: $(Bi, Pb)_2 \cdot Sr_2 CuO_{6+\delta}$ (Pb-2201 or Raveau phase, $T_c \approx 10$–15 K), $(Bi, Pb)_2 Sr_2 CaCu_2 O_{8+\delta}$ (Pb-2212 phase, $T_c \approx 85$–95 K) and $(Bi, Pb)_2 Sr_2 Ca_2 Cu_3 O_{10+\delta}$ (Pb-2223 phase, $T_c \approx 105$–115 K). As shown in Fig. 1, all these phases are contained in the isopleth defined by the index x in the formula $[(Bi, Pb)_2 Sr_2 CuO_6]_{1-x}$–$[Ca Cu O_2]_x$ $(0 < x < 1)$.

In our samples, part of the bismuth was substituted by lead with the intended compositions:

Pb-2212: $(Bi_{1.6} Pb_{0.4}) Sr_2 CaCu_2 O_{8+\delta}$

Pb-2223: $(Bi_{1.6} Pb_{0.4}) Sr_2 Ca_2 Cu_3 O_{10+\delta}$

in order to stabilize the 2223 phase.

Optimization of the processing of these superconducting phases requires a comprehensive study of the dependence of phase equilibria and phase stability in this system on temperature, chemical composition and oxygen pressure.

A number of recent works [1–5] showed an exchange of oxygen between the ceramics and the surrounding atmosphere during heating and cooling between 750 and 980°C. Satre et al. [4, 5] demonstrated the reversibility of such exchange. So, in the description of phase equilibria, the partial pressure of oxygen is a sensitive parameter.

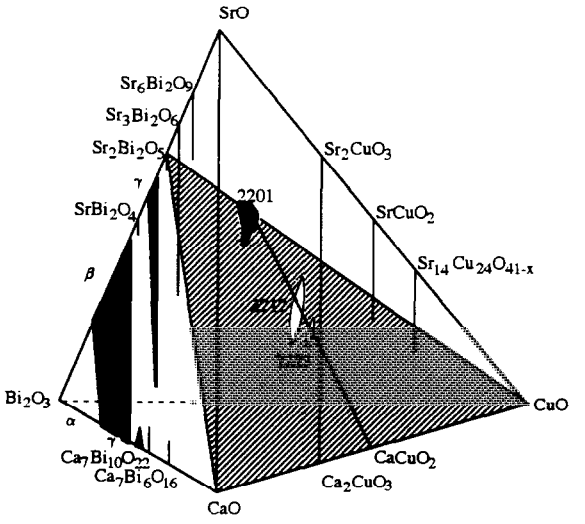

Fig. 1. Location of the studied phases in the quaternary system Bi_2O_3–SrO–CaO–CuO at 850°C in air.

According to the recent evaluation by Strobel et al. [6] (Fig. 2), the eutectoïd formation of the Pb-2223 phase from the Pb-2212, $(Sr, Ca)_2CuO_3$ and CuO phases was reported to be at about 835°C and it melts at 876°C. The 2212 phase melts at about 880°C. The melting point of the Raveau phase was determined to be about 900°C. Majewski [7] reports the lower stability temperature of the 2212 phase to be close to 660°C.

The purpose of the present paper is to investigate the phase transformations, by oxygen electromotive force and electrical resistance thermal analysis, in the Pb-2212 and Pb-2223 compositions.

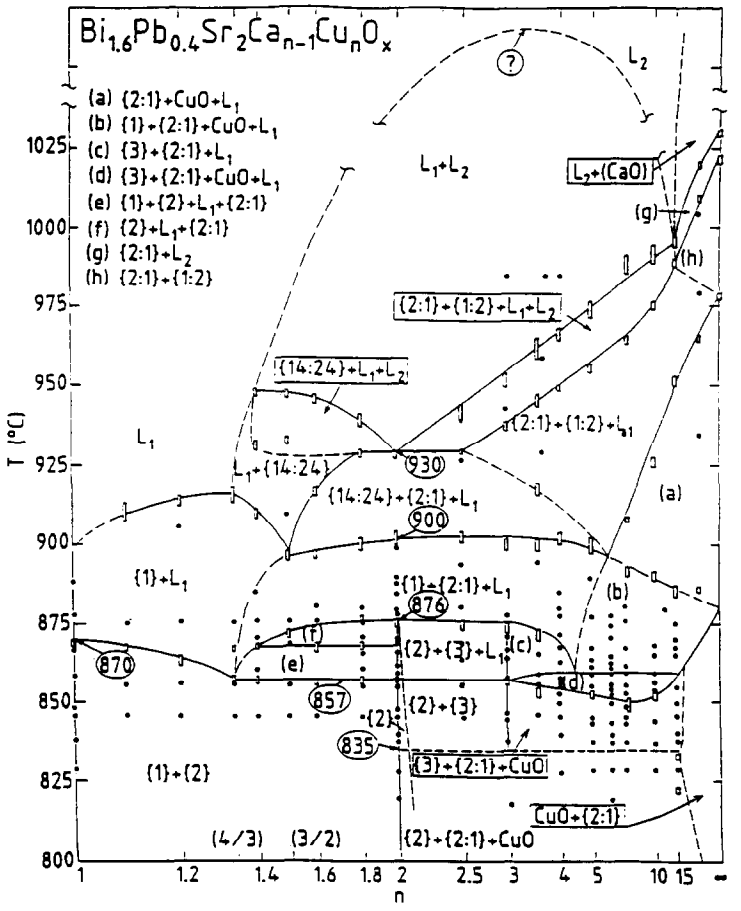

Fig. 2. The Strobel phase diagram for the line of compositions: $(Bi_{1.6}Pb_{0.4})Sr_2Ca_{n-1}Cu_nO_{2n+4+\delta}$[6]. {1}, {2} and {3} are the superconducting phases with one, two and three CuO_2 planes; they are denoted in the text by Pb-2201, Pb-2212 and Pb-2223, respectively.

2. Experimental

2.1. Samples preparation

The samples were synthetized by coprecipitation in an alkaline solution [8]. Aqueous nitrate solutions of Bi, Pb, Sr, Ca and Cu were mixed in stoichiometric proportions to obtain a 0.08 M aqueous solution and added to oxalic acid solution. The coprecipitation in alkaline solution was performed by means of an organic base (triethylamine). The oxalic acid and the triethylamine solutions were added simultaneously to the mixed aqueous solutions while stirring. The pH was kept at a constant value (pH $\approx$ 11). The green precipitate was filtered, dried at 80°C and submitted to pyrolysis up to 850°C, then studied by X-ray diffraction.

2.2. EMF measurements

For continuous monitoring of variations of oxygen activity by e.m.f. measurement, we employed an electrolytic cell using CaO-stabilized zirconia as an oxygen-conducting solid electrolyte. A schematic representation of the cell assembly is shown in Fig. 3. The sample was deposited in the $ZrO_2(CaO)$ crucible which separates two regions with different oxygen activities, although they are surrounded by the same atmosphere. The sample imposes its own oxygen activity, $a(O_2)$, on the internal face of the crucible by direct O^{2-} exchange between the condensed phases, whereas the surrounding gas imposes the reference oxygen activity, $a_{ref}(O_2)$, on the external face.

The relationship between e.m.f. (E) and the oxygen activity of the ceramics at the temperature T is given by the Nernst equation:

$$E = \frac{RT}{4F}\ln\left(\frac{a(O_2)}{a_{ref}(O_2)}\right)$$

where R and F are the gas and Faraday constants, respectively.

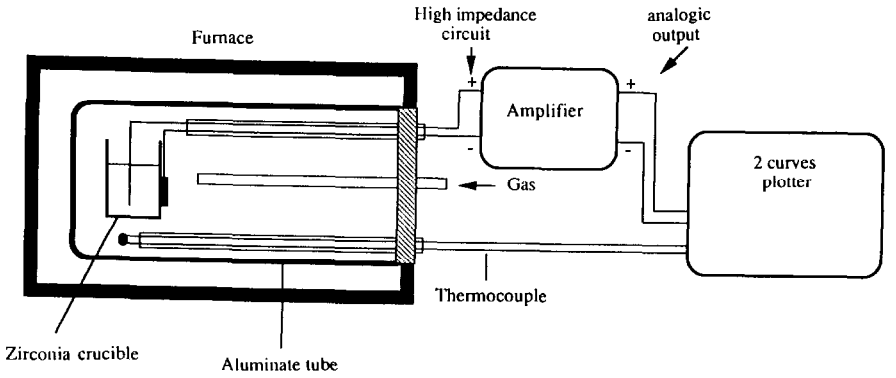

Fig. 3. Schematic diagram of cell assembly for e.m.f. measurement.

To carry out the e.m.f. measurements, one platinum wire was put in contact with the inner face of the crucible inside the ceramics and another was wound as a coil on the external face of the crucible as a reference electrode. The two conducting wires were connected for measurement with a digital voltmeter with an input impedance of 20 MΩ. The e.m.f. thermal analysis signal was recorded versus time for both increasing and decreasing temperature from room temperature to about 1000°C. The temperature was recorded simultaneously as another track on the same plot. A controlled mixture of pure oxygen and purified nitrogen ($p(O_2) \approx 5 \times 10^{-6}$ atm) flowed through the device. In many experiments the partial oxygen pressure was fixed at 10^5 Pa (1 atm).

2.3. Electrical resistance measurements

Measurements of electrical resistance versus temperature, were made using the four-wires method. Two platinum wires were put in simultaneous contact with the ceramics inside the crucible, each one connected to the outside device by two platinum leads. A Setaram EJP 30 stabilized current generator gave a constant current, I = 0.1 mA, which flowed through the ceramics and created a voltage, U, which is proportional to the ceramics' resistance, R. The resistance and temperature signals were plotted, versus time, on the same plotter. The two U and I circuits are independent (Fig. 4).

3. Results

3.1. Oxygen activity thermal analysis

First, the ceramics were heated to about 1000°C to obtain good chemical and conducting contact with the crucible.

During the following experiments, several heating–cooling cycles with rates between 3 and 6°C min^{-1} were carried out.

Our e.m.f. thermal analysis shows abrupt variations of the oxygen activity signal, versus temperature, and we observe different reversible peaks on heating and cooling in some temperature intervals where the sample exhibits a monovariant behaviour: $a(O_2) = f(T)$. These temperature domains correspond to some phase transitions in the material with $a(O_2) > a_{ref}(O_2)$ on heating and $a(O_2) < a_{ref}(O_2)$ on cooling indicating a reversible redox equilibrium. Between these domains, the cell response is approximately $E = 0$ mV corresponding to a polyvariant equilibrium where the oxygen pressure imposes its oxygen activity inside the material.

In Tables 1 and 2 we describe the e.m.f. experimental conditions and summarize the experimental results corresponding to the Pb-2212 and Pb-2223 compositions, respectively. We indicate the temperature of the observed peak maxima on heating and cooling, and the corresponding e.m.f. (E) and oxygen activity ($a(O_2)$) for several experiments (Fig. 5 and 6).

These results allowed us to determine the existence of some redox equilibria over the following temperature ranges:

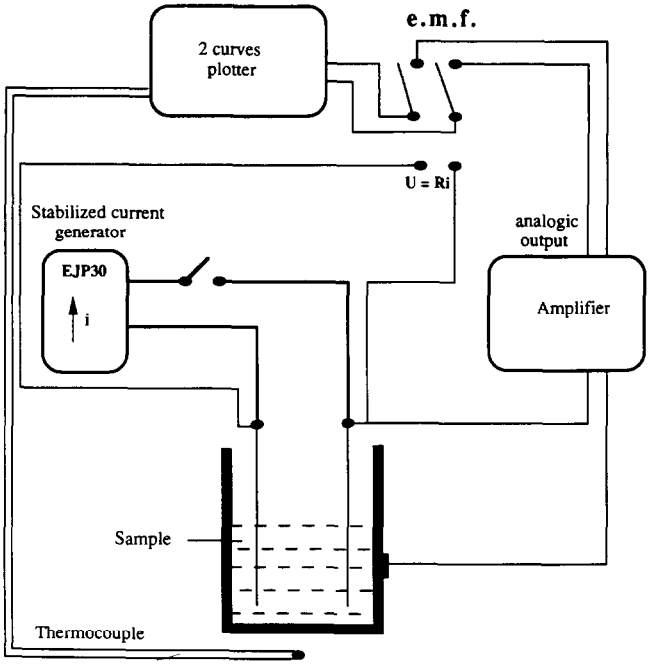

Fig. 4. Schematic diagram of cell assembly for electrical resistance measurement.

Pb-2212 composition:

(300–600, maximum ≈ 475°C)(715–800, maximum ≈ 750°C)(860–925°C)(925–945°C)

Pb-2223 composition:

(350–650, maximum ≈ 500°C)(700–800, maximum ≈ 725°C)(825–850°C)(860–870°C)(> 900°C)

The high temperature phase transitions are in good agreement with the phase diagram published by Strobel et al. [6]. This observation establishes the validity of this new method for thermal analysis.

3.2. *Electrical resistance thermal analysis*

To carry out thermal analysis of the electrical resistance signal versus temperature, several heating–cooling cycles were performed between room temperature and 700°C on both compositions: Pb-2212 and Pb-2223.

The curves plotted in Fig. 7 and Fig. 8 show a continuous decrease of resistance with increasing temperature up to 350°C. Above this temperature, the resistance exhibits an

Table 1
EMF thermal analysis of the Pb-2212 composition

Cycle	Experimental conditions	Peak maxima on heating			Peak maxima on cooling		
		T/°C	E/mV	$a(O_2)$/atm	T/°C	E/mV	$a(O_2)$/atm
	Heating from 440 to 970°C	525	+7.2	1.520	475	−16.5	0.359
	at 6°C min^{-1}.	760	+1.2	1.055	725	−9.4	0.646
Cycle 1	Cooling to 725°C at	890	+5.4	1.240	850	(slope wave)	
	4.4°C min^{-1}, then						
	the furnace imposes its	940	+2.0	1.080	925	0.3	0.988
	own cooling rate.						
	Heating from 415 to 750 at	505	+8.7	1.680	460	−11.6	0.480
	4.8°C min^{-1} then heating	760	+1.0	1.046	730	−9.6	0.641
Cycle 2	to 965°C with the furnace's	890	+5.4	1.240	850	(slope wave)	
	own heating rate.						
	Cooling at the furnace's	945	+2.4	1.096	930	−0.5	0.981
	own cooling rate.						
	Heating from 375 to 650°C	505	+2.8	1.182	460	−15.6	0.372
	then isothermal stage at				555	−14.6	0.441
Cycle 3	690°C for 18 h.	775	+2.6	1.122	730	−10.5	0.615
	From 690 to 930°C at 2°C min^{-1}.	890	+4.2	1.182	850	(slope wave)	
	Cooling at the furnace's						
	own cooling rate.	925	+1.6	1.064	905	−0.4	0.984
	Heating from 275 to 650°C	510	+4.0	1.307	475	−13.0	0.446
	at 3°C min^{-1}.						
	Isothermal stage at 650°C for						
	17 h.	760	+2.7	1.129	770	−9.8	0.647
Cycle 4	From 650 to 775°C at 3°C min^{-1}.	880	+5.0	1.223	850	(slope wave)	
	Cooling at the furnace's						
	own cooling rate.				935	−0.7	0.973
	Heating from 140 to 475°C						
	at 3°C min^{-1}.	510	+2.6	1.167	475	−15	0.394
Cycle 5	From 475 to 965°C	750	+0.4	1.018	750	−9.8	0.641
	at 3.5°C min^{-1}.	875	+5.3	1.239	850	(slope wave)	
	Cooling at the furnace's						
	own cooling rate.				925	−0.4	0.985

R plateau between 300 and 450°C both on heating and cooling for the Pb-2212 composition, and between 350 and 600°C both on heating and cooling for the Pb-2223 composition.

Then, the electrical resistance thermal analysis was carried out up to 950°C for the Pb-2212 composition. The curves obtained show various minima at around: 740–770°C, 875–890°C and 925–935°C (Fig. 9 and Table 3).

Table 2
EMF thermal analysis of the Pb-2223 composition

Cycle	Experimental conditions	Peak maxima on heating			Peak maxima on cooling		
		T/°C	E/mV	$a(O_2)$/atm	T/°C	E/mV	$a(O_2)$/atm
	Heating from 520 to 650°C	575	+10	1.728	485	−37.5	0.100
	at 1°C min^{-1}.	760	+5.7	1.292	740	−7.8	0.699
Cycle 1	Isothermal stage at 715°C.				815	−2.2	0.910
	From 715 to 935°C at 3.5°C min^{-1}	830	+6.0	1.287	830	−2.5	0.900
	Cooling: 935–800°C at 4.7°C min^{-1}	865	+4.3	1.192	865	−2.2	0.914
	800–675°C at 3.9°C min^{-1}.	900	+0.6	1.024	900	−1.3	0.950
	650–500°C at 3.5°C min^{-1}.						
	Heating from 475 to 650°C at						
	4.4°C min^{-1}.	575	+15	2.272	450	−50	0.048
	Isothermal stage at 700°C for 3 h	750	+6.2	1.325	745	−8.0	0.696
Cycle 2	From 700 to 940°C at 3.9°C min^{-1}	825	+5.8	1.278	850	−1.8	0.928
	Cooling at the furnace's	860	+4.2	1.188	865	−1.6	0.937
	own cooling rate	900	+0.5	1.020	900	−0.8	0.969
	Heating from 460 to 860°C						
	at 4.2°C min^{-1}.	585	+20	2.249	455	−40.2	0.077
		750	+3.8	1.188	750	−8.4	0.683
Cycle 3	Isothermal stage at 860°C for 3 h	810	+2.3	1.103	800	−4.0	0.841
	Cooling at the furnace's	830	+2.0	1.125	850	−1.0	0.959
	own cooling rate.	865	+3.7	1.163	870	−0.9	0.964
		900	+1.0	1.040	900	−0.5	0.980

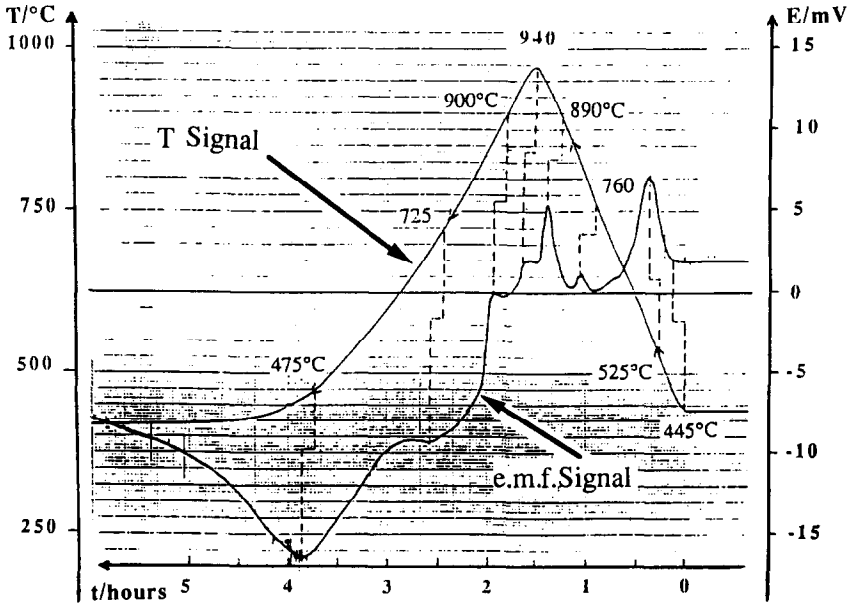

Fig. 5. Example of e.m.f. thermal analysis for the Pb-2212 composition.

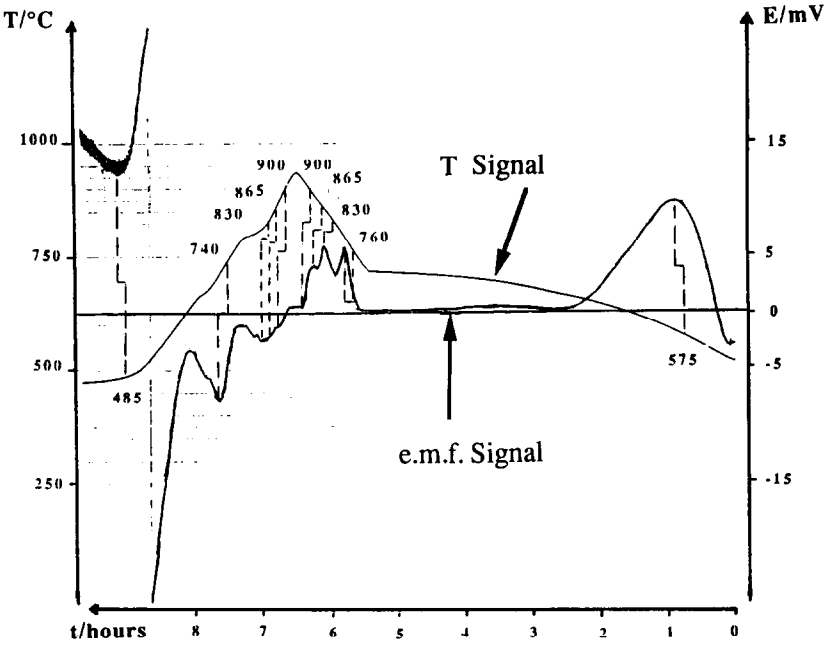

Fig. 6. Example of e.m.f. thermal analysis for the Pb-2223 composition.

4. Discussion

We notice that our e.m.f. and electrical resistance thermal analysis fit together, and in the light of the Strobel et al. phase diagram [6], we can establish parallelism in the behaviour of the Pb-2212 and Pb-2223 compositions (Tables 4 and 5).

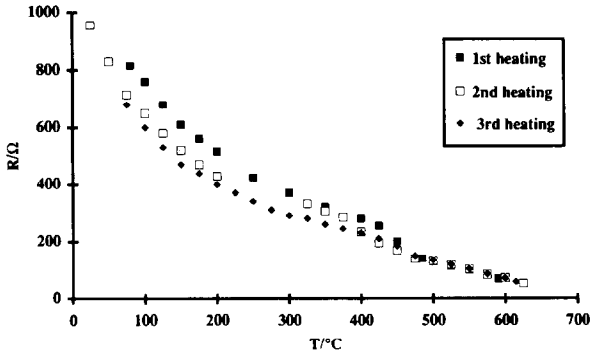

Fig. 7. Plot of electrical resistance against temperature for the Pb-2212 composition: a, on heating; b, on cooling.

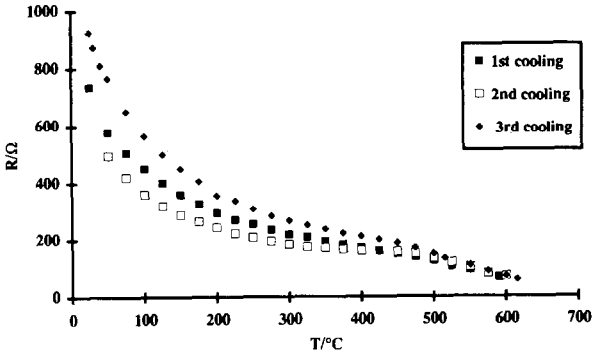

Fig. 7b

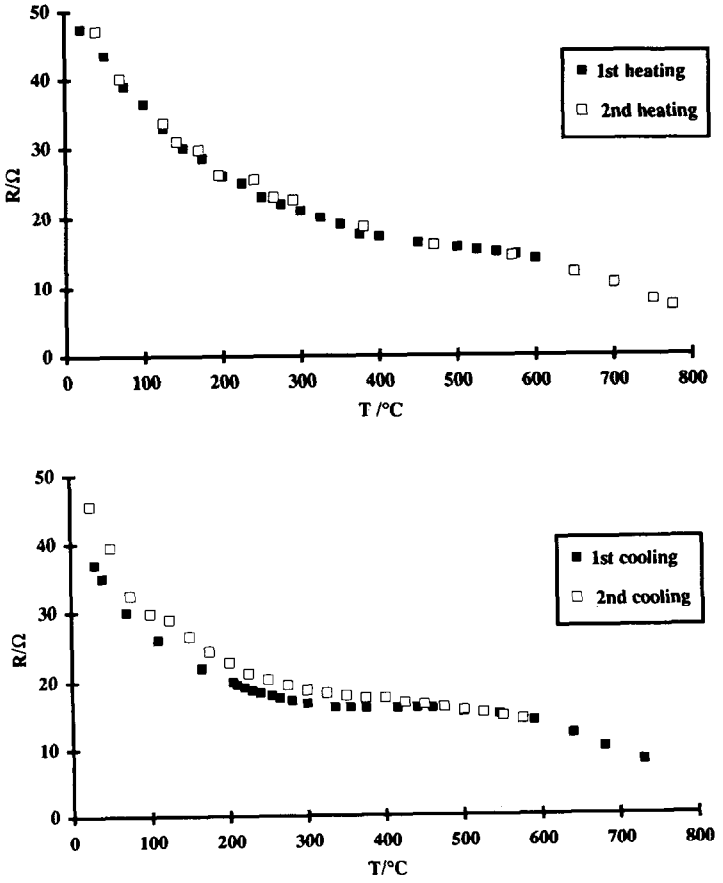

Fig. 8. Plot of electrical resistance against temperature for the Pb-2223 composition: a, on heating; b, on cooling.

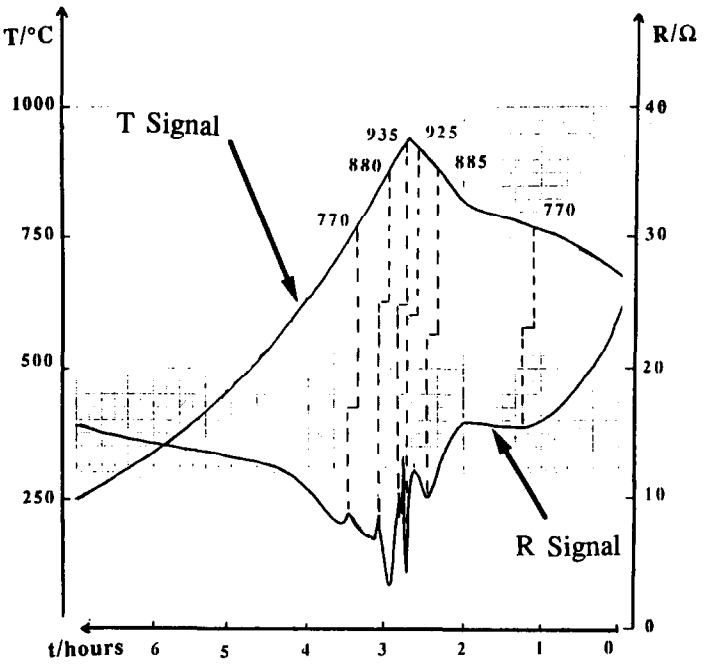

Fig. 9. Example of electrical resistance thermal analysis at high temperature for the Pb-2212 composition.

Table 3
Electrical resistance thermal analysis of the Pb-2212 composition

Cycle	Experimental conditions	Peak maxima on heating	Peak maxima on cooling
	Heating from 25 to 490°C	760°C	–
	at 4.5°C min^{-1}.	880°C	–
Cycle 1	From 500 to 750°C at 3.5°C min^{-1}	anomalies at	–
		900, 925 and	–
	and to 1025°C at 1.5°C min^{-1}	1000°C	–
	Heating from 325 to 575°C at 2.5°C min^{-1}	770°C	770°C
	From 675 to 800°C at 1.5°C min^{-1}	885°C	880°C
Cycle 2	From 810 to 940°C at 2.5°C min^{-1}	925°C	935°C
	Cooling at the furnace's		
	own cooling rate.		
	Heating from 25 to 525°C at 4°C min^{-1}.	750°C	750°C
	Isothermal stage at 525°C for 90 min	885°C	875°C
Cycle 3	From 525 to 750°C at 3.5°C min^{-1}	925°C	925°C
	From 750 to 950°C at 2.5°C min^{-1}	935°C	
	Cooling at the furnace's		
	own cooling rate.		
	Heating from 25 to 375°C at 3.5°C min^{-1}	740°C	750°C
	375 to 625°C at 2.5°C min^{-1}	870°C	875°C
Cycle 4	625 to 950°C at 1.5°C min^{-1}	925°C	920°C
	Cooling at the furnace's	935°C	
	own cooling rate		

4.1. High temperature phase transformations

The high temperature peaks observed in both e.m.f. and electrical resistance thermal analysis can be easily interpreted. For the Pb-2212 composition, the peak at 875–890°C consists mainly of the melting of the Pb-2212 superconducting phase, and the peak observed at 925–945°C is ascribed to the melting of the $(Sr, Ca)_2Cu_1O_3$ (denoted {2:1}) phase (Fig. 10; see X-ray pattern at equilibrium temperature). For the Pb-2223 composition, the peak detected at 825–830°C corresponds to the eutectoïd formation of the Pb-2223 phase starting from the Pb-2212, Ca_2CuO_3 and CuO phases, whereas the peak at 860–870°C represents the melting of this Pb-2223 phase. The peak observed at 900°C can be attributed to the melting of the Raveau phase.

Table 4
Correspondence between our thermal analysis results and the Strobel phase diagram [6] for the Pb-2212 composition

Electrical resistance thermal analysis	Strobel phase diagram [6]	EMF thermal analysis
Plateau:300–450°C	Not mentioned	Redox peak between 400 and 700°C.
Minima at 740–775°C	Not mentioned	Redox peak maximum between 725 and 760°C.
Minima at 875–890°C	Melting of the Pb-2212 phase at 876°C	Redox peak maximum at 890°C.
Anomaly at 900°C (in one experiment)	Melting of the Pb-2201 phase at 900°C.	Not detected
Minima at 925–935°C	Eutectic melting of {14:24} and {2:1} phases at 930°C.	Redox plateau at 925–945°C.

Table 5
Correspondence between our thermal analysis results and the Strobel phase diagram [6] for the Pb-2223 composition

Electrical resistance thermal analysis	Strobel phase diagram [6]	EMF thermal analysis
Plateau: 300–600°C	Not mentioned	Redox peak between 450 and 700°C
	Not mentioned	Redox peak maximum between 740 and 760°C.
	Eutectoïd formation of the Pb-2223 phase at 835°C	Redox peak maximum at 825–830°C.
	Melting of the Pb-2223 phase at 876°C.	Redox peak maximum at 860–870°C.
	Melting of the Pb-2201 phase at 900°C.	Redox peak maximum at 900°C.

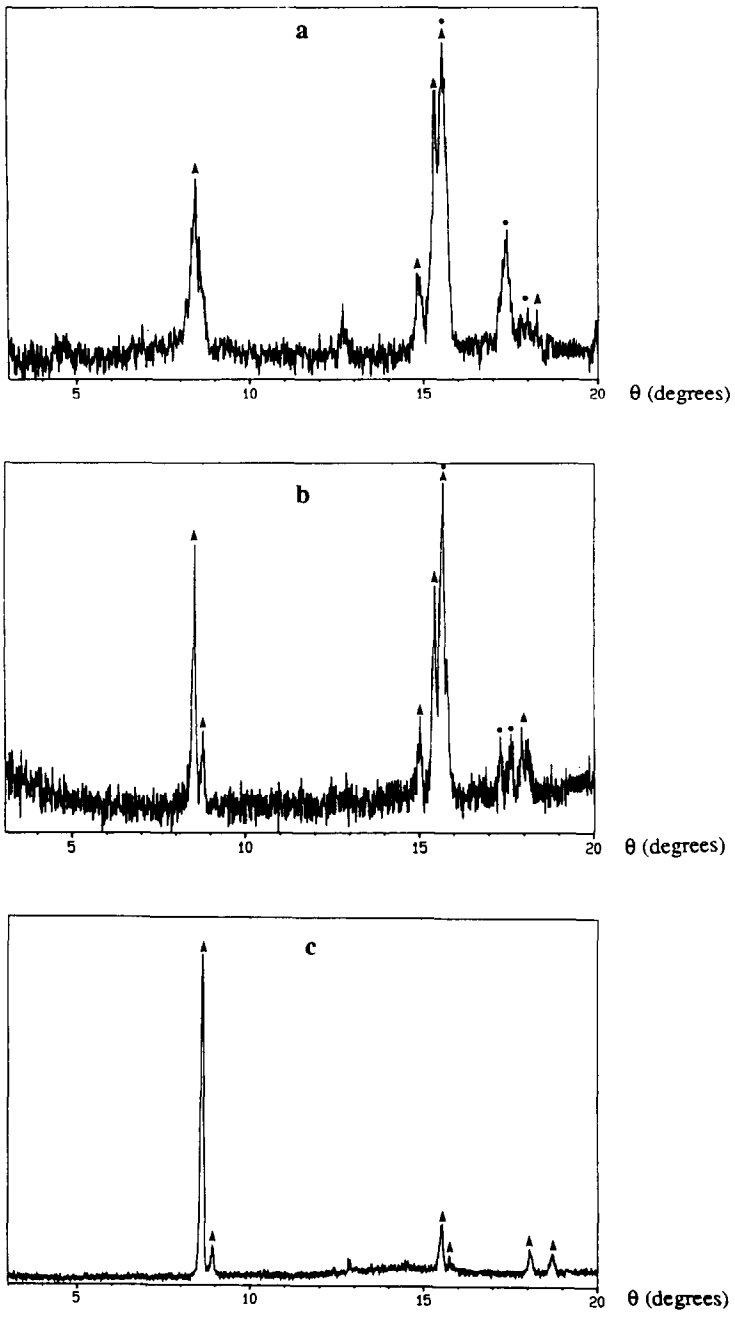

Fig. 10. X-ray diffraction pattern at equilibrium temperature under a $p(O_2) = 80\,kPa$ gas atmosphere and showing the melting of the $(Sr,Ca)_2Cu_1O_3$ (denoted {2:1}) phase between 925 and 940°C (●, {2:1} phase; ▲, $(Sr,Ca)_2PbO_4$ phase): a, 910°C; b, 925°C; c, 940°C.

4.2. Low temperature phase transformations

For both compositions, below 800°C, two reversible e.m.f. thermal analysis peaks were observed in the temperature ranges 700–800°C and 300–650°C. These correspond to new transformations in these compositions which were also detected by electrical resistance thermal analysis (Table 4).

Using X-ray diffraction we have tried to attribute the first peak observed near 750°C either to the Majewski eutectoïd reaction: $2212 \leftrightarrow 2201 + 1/2\,Ca_2CuO_3 + 1/2\,CuO$ or to the precipitation of the $(Ca, Sr)_2PbO_4$. But X-ray patterns realised inside a heating Anton–Paar camera [9] show no any evidence of transformation below 820°C.

It can also be assumed that both these transformations, observed at temperatures of approximately 750°C and 500°C can be attributed to a valence change in the Raveau, Pb-2212 or Pb-2223 phases.

5. Conclusion and tentative explanations

Phase transformations in the $[(Bi, Pb)_2Sr_2CuO_6]_{1-x}$–$[CaCuO_2]_x$ $(0 < x < 1)$ isopleth were investigated from room temperature to 950°C, by oxygen activity and electrical resistance thermal analysis inside an electrolytic cell of CaO-stabilized zirconia.

This study enabled us to show that oxygen activity is a sensitive parameter for determining, by thermal analysis, the phase transitions in high T_c superconducting ceramics.

By these two methods of thermal analysis, we have confirmed the main known phase transformations in the Pb-2212 and Pb-2223 compositions: the eutectoïd formation of the Pb-2223 phase at 825–830°C, the melting of the Pb-2223 phase at 860–870°C, the melting of the Pb-2212 phase between 875 and 890°C, the melting of the Raveau phase at 900°C and the melting of the $(Sr, Ca)_2Cu_1O_3$ (denoted {2:1}) phase near 930°C.

Two new redox phenomena close to 750°C and 500°C under $p(O_2) = 10^5$ Pa were detected both by e.m.f. and resistance thermal analysis, without any evidence of structural phase transition. Valence change of some cations inside the high T_c superconducting phases can be expected in the temperature ranges where reversible redox equilibria are observed without modification of the X-ray pattern. $Pb^{4+} \Leftrightarrow Pb^{2+}$ and $Bi^{3+} \Leftrightarrow Bi^{5+}$ could be hypothetical candidates for such valence transitions, in particular around 500°C. Some recent chemical test of reactivity of the Pb-2212 powder, with Mn^{2+} acid solution, has proved that, after heat treatment at low temperature and cooling, the Pb-2212 composition is able to oxidise Mn^{2+} to Mn^{7+}, (colorimetric test). This recent result indicates that, after such heat treatment, the ceramics contains either Pb^{4+} or Bi^{5+} cations.

References

[1] L.M. Rubin, T.P. Orlando, J.B. Van der Sande, G. Gorman, R. Savoy, R. Swope and R. Beyers, Appl. Phys. Lett., 61 (1992) 1977.
[2] R.O. Suzuki, P. Bohac and L.J. Gauckler, J. Am. Ceram. Soc., 75 (1992) 2833.
[3] T. Konai and T. Kamo, Supercond. Sci. Technol., 6 (1993) 510.

[4] P. Satre, A. Sebaoun, O. Monnereau and G. Vacquier, J. Phys. III (France), 4 (1994) 261.
[5] P. Satre and A. Sebaoun, J. Therm. Anal., 41 (1994) 211.
[6] P. Strobel, J.C. Tolédano, D. Morin, J. Schneck, G. Vacquier, O. Monnereau, J. Primot and T. Fournier, Physica C, 201 (1992) 27.
[7] P. Majewski, Adv. Mater., 6 (1994) 465.
[8] M. Mansori, P. Satre, C. Breandon, M. Roubin and A. Sebaoun, Ann. Chim. Fr., 18 (1993) 537.
[9] M. Mansori, Thèse, Université de Toulon et du Var, 10 novembre 1995.